PROTEINS
STRUCTURE ■ FUNCTION ■ BIOINFORMATICS

Is there nascent structure in the intrinsically disordered region of troponin I?

Olivier Julien,[1] Pascal Mercier,[1] Claire N. Allen,[2] Olivier Fisette,[3] Carlos H. I. Ramos,[4] Patrick Lagüe,[3] Tharin M. A. Blumenschein,[2] and Brian D. Sykes[1]*

[1] Department of Biochemistry, University of Alberta, Edmonton, AB, Canada
[2] School of Chemistry, University of East Anglia, Norwich, United Kingdom
[3] Département de biochimie et de microbiologie, Université Laval, Québec, QC, Canada
[4] Chemistry Institute, University of Campinas UNICAMP, Campinas SP, Brazil

ABSTRACT

In striated muscle, the binding of calcium to troponin C (TnC) results in the removal of the C-terminal region of the inhibitory protein troponin I (TnI) from actin. While structural studies of the muscle system have been successful in determining the overall organization of most of the components involved in force generation at the atomic level, the structure and dynamics of the C-terminal region of TnI remains controversial. This domain of TnI is highly flexible, and it has been proposed that this intrinsically disordered region (IDR) regulates contraction via a "fly-casting" mechanism. Different structures have been presented for this region using different methodologies: a single α-helix, a "mobile domain" containing a small β-sheet, an unstructured region, and a two helix segment. To investigate whether this IDR has in fact any nascent structure, we have constructed a skeletal TnC-TnI chimera that contains the N-domain of TnC (1–90), a short linker (GGAGG), and the C-terminal region of TnI (97–182) and have acquired ^{15}N NMR relaxation data for this chimera. We compare the experimental relaxation parameters with those calculated from molecular dynamic simulations using four models based upon the structural studies. Our experimental results suggest that the C-terminal region of TnI does not contain any defined secondary structure, supporting the "fly-casting" mechanism. We interpret the presence of a "plateau" in the ^{15}N NMR relaxation data as being an intrinsic property of IDRs. We also identified a more rigid adjacent region of TnI that has implications for muscle performance under ischemic conditions.

Proteins 2011; 79:1240–1250.

Key words: NMR; muscle regulation; protein dynamics; molecular dynamics; NMR relaxation.

INTRODUCTION

Human skeletal, cardiac, and smooth muscles all produce force in a similar manner and all are calcium regulated. For the striated muscle found in skeletal and cardiac muscle tissues, the sarcoplasmic calcium concentration dictates the activation or inhibition of the contractile machinery through the troponin complex. Troponin is composed of three structural subunits found in an equimolar ratio. Troponin C (TnC) is the calcium-binding subunit, which senses changes in the cellular calcium concentration. Troponin T (TnT) is the tropomyosin-interacting subunit that serves as an anchor to position the troponin complex in place on the thin filament. Troponin I (TnI) is the inhibitory subunit, which modulates the actomyosin ATPase activity by binding to actin (for reviews, see Refs. 1–4).

When calcium binds to TnC, a structural conformational change occurs in the N-terminal domain of TnC, which leads to the binding of the "switch" region of TnI (sSp) and subsequent release of TnI from actin. The resulting movement of tropomyosin exposes myosin-binding sites on actin, resulting in the power stroke. Although many structural studies of the muscle system have been successful in determining the overall organization of most of the components involved in force generation at the atomic level, the structure and dynamics of TnI remains controversial. Specifically, the C-terminal region of TnI (residues 97–182) has been the focus of many studies (discussed below), but a clear picture of the structure, dynamics, and function of this region remains unclear. This domain of TnI is highly flexible, and it has been proposed that this intrinsically disordered region (IDR) regulates contraction via a "fly-casting" mechanism.[5–7]

Grant sponsor: The Wolfson Foundation; Grant sponsor: Canadian Institutes of Health Research (CIHR) Grant sponsor: NANUC; Grant sponsor: The Natural Science and Engineering Research Council of Canada (NSERC); Grant sponsor: Alberta Heritage Foundation for Medical Research (AHFMR) (Dr. Lionel E. McLeod Health Research Scholarship); Grant sponsor: CIHR (Frederick Banting and Charles Best Canada Graduate Scholarship)
*Correspondence to: Brian D. Sykes, Department of Biochemistry, 4-19 Medical Sciences Building, University of Alberta, T6G 2H7 Edmonton, Canada. E-mail: brian.sykes@ualberta.ca.
Received 5 October 2010; Revised 20 November 2010; Accepted 27 November 2010
Published online 13 December 2010 in Wiley Online Library (wileyonlinelibrary.com).
DOI: 10.1002/prot.22959

The focus of this article is the skeletal C-terminal region of TnI (sTnI), because of its important role in the regulation of muscle contraction. For example, many familial hypertrophic cardiomyopathy mutations occur in this region.[8] In a previous study of the 52 kDa troponin complex by nuclear magnetic resonance (NMR) spectroscopy, we recognized the C-terminal region of sTnI as having the characteristics of an IDR and probed the dynamics of this region in presence and absence of calcium.[6] Our results indicated that this region is highly flexible based on NMR relaxation data and chemical shifts. Similar results have also been observed for cardiac TnI.[9] Interestingly, we observed a "plateau" in the relaxation data in the middle of the IDR of TnI, which we interpreted as a possible indication of some nascent structure.

The question remains: is there a nascent structure in the C-terminal region of TnI? Different structures have been presented over the years for this region using different methodologies: a long single α-helix has been observed by X-ray crystallography in the structure of the cardiac troponin complex,[10] a "mobile domain" containing a small β-sheet flanked by two short α-helices was determined using solution NMR,[11] two antiparallel helical segments were modeled to fit SANS and SAXS data,[12] and a mainly unstructured region proposed from NMR relaxation and chemical shifts,[6] further supported by the absence of electronic density for residues 144–182 of TnI in the X-ray structure of skeletal troponin.[13] It is important to mention that all these studies were done in the off-state, when TnI is bound to TnC and removed from actin. The dynamics has also been probed bound to actin using SDSL-EPR spectroscopy.[14] The question of whether there is in fact any structure, nascent or otherwise, in this region of TnI is the focus of this article.

To avoid the experimental constraints created by the size of the troponin complex, we have constructed a skeletal TnC-TnI chimera to study the structure and dynamics of the regulatory region of troponin, combining the skeletal N-terminal domain of TnC (sNTnC) and the C-terminal region of TnI (sTnI) in a single polypeptidic chain.[15] The sequence of the skeletal TnC-TnI chimera contains 181 amino acids; it starts with a methionine due to the expression system (omitted in the numbering), followed by residues 1 to 90 of sTnC linked by a short GGAGG flexible linker to residues 98 to 182 of sTnI. When the TnI portion of the chimera is discussed in the text, it is referred to as residues 98–182 to agree with the human skeletal TnI sequence numbering. The use of this 20 kDa construct has many advantages over the 52 kDa ternary troponin complex, avoiding problems with limited stability, solubility, aggregation, and the rigid requirement of the equimolar ratios of the different subunits for the proper assembly of the ternary complex in solution. The use of high-salt concentrations (250 m*M*) in previous studies could possibly have lead to apparent IDR, and the use of ^{2}H labeling might have altered the stability of the complex. The increased stability of the chimera makes it easier to study under a variety of conditions. The chimera has also been previously shown to be functional, capable of regulating actomyosin ATPase.[15]

We have assigned the backbone chemical shifts of the chimera (142 out of 180 residues) and measured backbone amide ^{15}N NMR relaxation data. Experimental relaxation parameters were compared with those calculated from molecular dynamic simulations using four models for the structure of the chimera (Fig. 1), based on the previous structural studies mentioned above. We conclude that none of the secondary structure models proposed so far for the C-terminal region of TnI is correct in solution. This region is likely an IDR, although the molecular dynamic simulations were unable to accurately reproduce the large motions of an IDR. The chimera is an authentic mimic for the study of the "structure" and dynamics of the C-terminal region of TnI, because the chemical shifts and relaxation data for both the TnC and TnI regions are unperturbed compared with the same regions in the core troponin complex.

MATERIALS AND METHODS

Sample preparation

Uniformly [^{15}N]- or [^{15}N, ^{13}C]-labeled skeletal TnC-skeletal TnI chimera was expressed as described[15] from the plasmid pET3aTnC (1–91)-TnI (98–182), but with the addition of 0.8 m*M* IPTG instead of lactose. Purification procedures were adapted from Tiroli *et al.*[15] Cells were lysed by sonication, followed by centrifugation for 3 h 20 min at 18,500 rpm at 4°C in a Beckman Avanti centrifuge, rotor JA20 (Palo Alto, CA). The supernatant was dialyzed against 100 m*M* acetate buffer, pH 5.0, 1 m*M* $CaCl_2$, 50 m*M* NaCl and centrifuged for 20 min at 18,500 rpm at 4°C in a Beckman Avanti centrifuge, rotor JA20. The soluble fraction was loaded into a HiTrap Q column (GE Healthcare) equilibrated with the same buffer. The chimera was eluted in the flow through. NMR samples were prepared in 90% H_2O/10% D_2O, 100 m*M* KCl, 10 m*M* Imidazole, 1 m*M* $CaCl_2$, 0.03% sodium azide, and 0.2 m*M* 2,2-dimethyl-2-silapentane-5-sulfonic acid. The pH was adjusted to 6.8 according to the frequency of the imidazole signal.[16]

NMR spectroscopy

NMR spectra were collected at 30°C (unless specified otherwise). Varian Inova 600 and 800 MHz, and Bruker Avance III 800 MHz NMR spectrometers equipped with triple resonance probes with Z-pulsed field gradients and a computer-controlled variable temperature (VT) module to regulate the temperature were used in this study. The 1D ^{1}H spectra were processed and plotted with VnmrJ 2.1B. The 2D and 3D spectra were all processed with

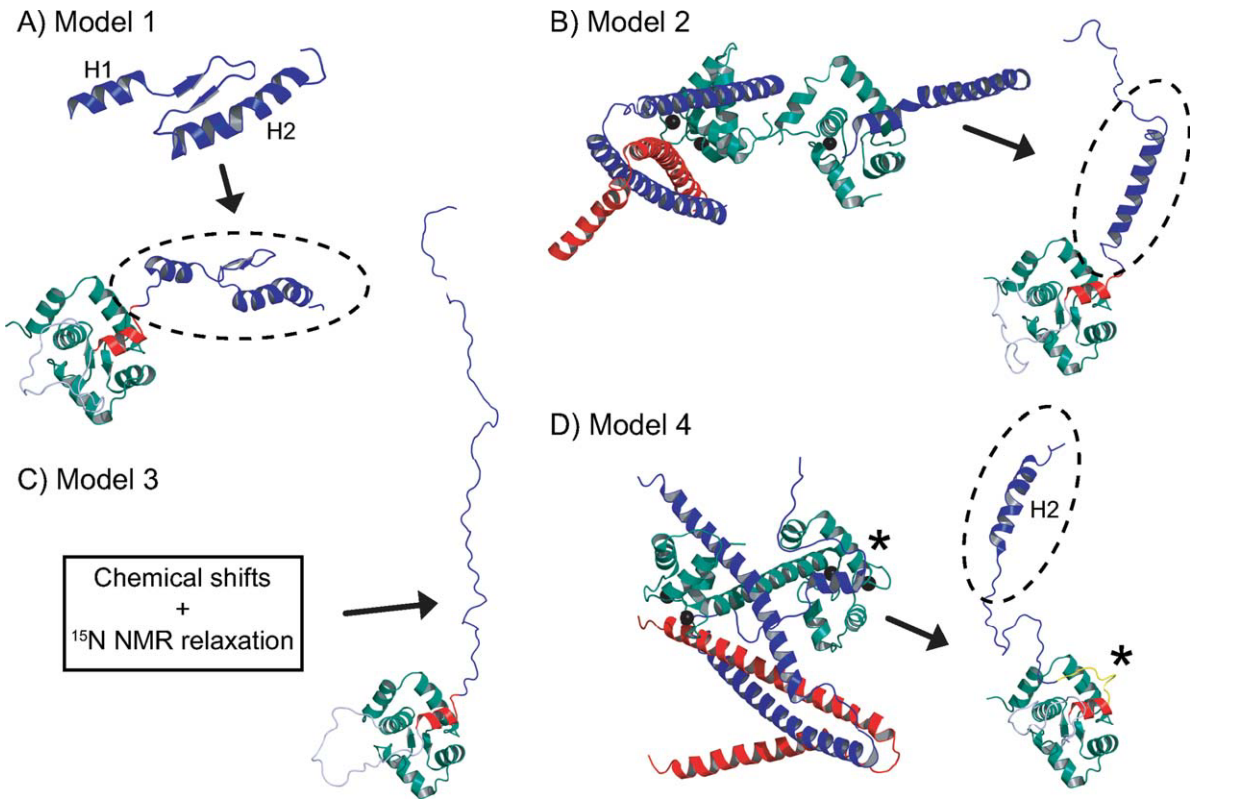

Figure 1

Four plausible models for the skeletal TnC-TnI chimera based on different TnI conformations. **A**: Model 1, based on the reported NMR structure of the C-terminal region of TnI determined by Murakami *et al.*[11] **B**: Model 2, based on the X-ray structure of the cardiac troponin complex determined by Takeda *et al.*[10] **C**: Model 3, based on the NMR relaxation data obtained by Blumenschein *et al.*[6] **D**: Model 4, based on the X-ray structure of the skeletal troponin complex,[13] featuring an interaction between residue H130 of sTnI and E20 of sTnC known as "histidine button."[32,33]

NMRPipe[17] and analyzed with NMRViewJ (One Moon Scientific). The relaxation data at 600 and 800 MHz were analyzed with the rate analysis module of NMRViewJ (v8.0-rc17).

A temperature series (from 5 to 50°C) was performed on a [^{15}N]-labeled sample at 600 MHz. One-dimensional ^{1}H and 2D ^{1}H-^{15}N HSQC NMR spectra were acquired at each temperature. The spectra were acquired with the water and gNhsqc pulse sequences of Biopack (Varian), respectively. The 1D spectra were acquired with a spectral width of 14 ppm, 128 transients, a relaxation delay of 1 s and an acquisition delay of 2 s. The ^{1}H-^{15}N HSQC were acquired with 16 transients, a relaxation delay of 1 s, and spectral widths of 14 ppm (ω_2) and 40 ppm (ω_1) with 2048 and 192 complex points, respectively. The 3D CBCACONH and HNCACB were acquired at 800 MHz with a relaxation delay of 1 s, spectral widths of 15 ppm (ω_3), 30 ppm (ω_2), and 75 ppm (ω_1) with 2048, 64 (or 42), and 164 (or 128) complex points, respectively. The 3D HNCACO and HNCO were acquired at 800 MHz with a relaxation delay of 1 s, spectral widths of 15 ppm (ω_3), 30 or 36 ppm (ω_2), and 36 ppm (ω_1) with 2048, 64, and 164 (or 192) complex points, respectively. To complete the chemical shifts assignment, a 3D ^{15}N NOESYHSQC was also acquired at 800 MHz, with a relaxation delay of 1.2 s, a mixing time of 0.1 s, spectral widths of 15 ppm (ω_3), 10 ppm (ω_2), and 40 ppm (ω_1) with 2048, 184, and 116 complex points, respectively.

Backbone amide relaxation data

All backbone amide relaxation data (^{15}N-T_1, ^{15}N-T_2 and {^{1}H}^{15}N-NOE) were measured from a series of 2D ^{1}H-^{15}N HSQC spectra acquired at both 600 and 800 MHz at 30°C. The relaxation experiments were all acquired with spectral widths of 15 ppm (ω_2) and 40 ppm (ω_1), and with 2048 (t_1) × 192 (t_2) complex points and 2048 (t_1) × 128 (t_2) complex points at 600 and 800 MHz, respectively. The T_1 relaxation delays were (10, 100, 200, 500, 750, 1000, 2000, and 3000 ms) at 600 MHz and (20, 100, 200, 500, 750, 1000, 2000, 3000, and 5000 ms) at 800 MHz. For ^{15}N-T_2 measurements, the relaxation delays were set to (10, 50, 90, 130, 170,

210, and 250 ms) at 600 MHz and (17, 51, 85, 136, 170, 214, and 255 ms) at 800 MHz. At 600 MHz, the delay between repetitions of the pulse sequence was 4 s for both ^{15}N-T_1 and ^{15}N-T_2. The NOE were measured in the absence and presence of proton saturation (5 s at 600 MHz, 6 s at 800 MHz).

Computational methods

The *CHARMM* program,[18] version c35b1, was used to build all four troponin hybrid TnC-TnI systems and perform simulations. Initial coordinates for each model were obtained by modeling residues 1–180 of the chimera using different published and deposited protein structures of the troponin system, or structural information of the Tn complex. The program modeler was used to generate starting coordinates.[19] For the four models presented in Figure 1, the sTnC portion of the chimera was modeled using both the structure of sNTnC in the X-ray structure of the skeletal Tn complex (PDB ID 1YTZ), as well as the NMR structure of sNTnC in complex with residues 115–131 of sTnI with a bifunctional rhodamine probe attached on the C helix of sTnC (PDB ID 1NPQ). For the sTnI portion of the chimera, the starting structures were built as follow. Model 1 [Fig. 1(A)] is based on a solution NMR structure of the C-terminal region of TnI.[11] This structure, known as the mobile domain, contains a two-stranded antiparallel β-sheet flanked by two α-helices (PDB ID 1VJD). Model 2 [Fig. 1(B)] is derived from the crystallographic X-ray structure of the cardiac troponin complex (10), and exhibits a long α-helix followed by a short disordered region as seen in one of the two presented conformers presented (PDB ID 1JLE). Model 3 [Fig. 1(C)] contains no restraints for sTnI portion of the chimera, based on the chemical shifts and NMR relaxation data for the skeletal Tn complex (6). Model 4 [Fig. 1(D)] is derived from the crystal structure of the skeletal troponin complex where residues 126–143 of sTnI in the structure of the sTn complex are disordered, but electronic density is observable in one of the two conformers presented (PDB ID 1YTZ).[13] The structure of this region highlights the interaction between residues 125–132 of sTnI with α-helix A of sTnC. In this model, we have included the H2 helix of the "mobile domain" (Model 1) to assess the possibility of a short α-helix as suggested by our chemical shift data, and ESR data for the homologue region of TnI in the cardiac system that becomes more ordered when binding to actin in the "on" state.[14]

Crystallographic water and ions were removed from all models. Hydrogen positions were computed using *CHARMM*'s hbuild routines. The initial protonation state of acid-base residues was determined using Poisson-Boltzman calculations and the *CHARMM* pbeq module[20] with the recommended protocol. The protein dielectric constant was set to 5, and a value of 80 represented the bulk solvent. All residues showed standard protonation states at a pH of 7.0. Calcium atoms, two per system, were placed in each calcium-binding domain, for a total system size of 2817 atoms.

Langevin dynamics were carried out using the CHARMM22 forcefield[21] with φ, ψ cross-term map correction (CMAP),[22] a leapfrog integrator, and one femtosecond timestep. The Generalized Born with a simple switching (GBSW) implicit solvent model[23] was used with the recommended settings: 0.6 Å smoothing length, 0.03 kcal/mol/Å^2 nonpolar surface tension coefficients, 1.5 Å grid spacing and the optimized radii from the GBSW module. The nonbonded interaction cut-off for both Van der Waals and electrostatics was set to 20 Å and smoothed up to 16 Å using a switching function. The length of bonds involving hydrogen atoms was constrained with the SHAKE algorithm.[23] The Langevin temperature bath was set to 25°C, with a 5.0°C allowed temperature deviation. Before dynamics proper, initial velocities were assigned randomly at −70°C; the system was then heated progressively to 25°C over 100 ps, and equilibrated for 4900 ps. Production runs were then recorded, one 20 ns trajectory (or more) for each model, with coordinates saved every picosecond.

The stability of the simulation was assessed from total system energy and backbone RMSD excluding the flexible domain, both of which were stable after about 1 ns, well under the equilibration time. The CHARMM NMR module was used to compute the NMR relaxation parameters (^{15}N-T_1, ^{15}N-T_2 and {^{1}H}^{15}N-NOE). Before analysis, global rotation and translation were removed by an RMSD-minimizing superposition, taking into account only residues located in α-helices and β-strands in the TnC moiety. Therefore, only local TnI motions are considered. Relaxation times were calculated for a spectrometer frequency of 600 MHz using a 10 ns global tumbling time (estimated from molecular weight, τ_c(ns) ∼ MW (kDa)/2) and a chemical shift anisotropy of 160 ppm for the ^{15}N nucleus. The correlation functions for the molecular motions[24] were computed over 75% of the time domain of the trajectory length. Order parameters (S^2) were computed as the value of the autocorrelation functions at 15 ns.

RESULTS

The residues 1–90 of the chimera correspond to the regulatory domain of sTnC (methionine from the expression system omitted), residues 91–95 are the GGAGG linker, and residues 96–180 correspond to residues 98–182 of the C-terminal portion of sTnI. When the sTnI portion of the chimera is discussed in the text, it is referred to as residues 98–182 to agree with the human skeletal TnI sequence numbering.

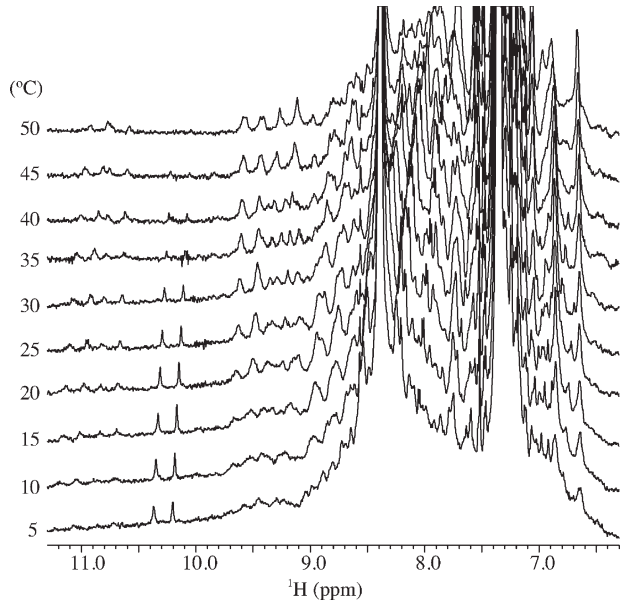

Figure 2

1D NMR spectra of the skeletal TnC-TnI chimera acquired at different temperatures. The stack plot shows the line width dependency of the aromatic and amide regions. The peaks get narrower around 30–35°C. As the temperature increases, one can notice the disappearance of the Trp ^{1}H-^{15}N indole signal (doublet at 10.3 ppm). The spectra were recorded on a 600 MHz NMR spectrometer.

Chemical shift assignment

Temperature series performed to determine the optimal temperature that should be used for the acquisition of the 3D spectra. On the one hand, higher temperatures allow for faster tumbling of the chimera in solution, which translate into narrower line widths. On the other hand, any nascent structure might get denatured at higher temperatures. A stacked plot of the 1D ^{1}H-^{15}N HSQC spectra is showed in Figure 2. We choose to study at 30°C where virtually all of the previous NMR data has been acquired. The 2D ^{1}H-^{15}N HSQC NMR spectrum acquired at 30°C is presented in Figure 3(A) and shows the assignments of the amide cross-peaks. The spectrum is well resolved, and virtually all expected resonances are present. Figure 3(B) shows a superimposition of reconstructed ^{1}H-^{15}N HSQCs based on the chemical shifts of the chimera and the respective domains of TnC[25] and TnI[11] in the Tn complex. The chemical shifts were globally adjusted to compensate for the TROSY acquisition mode and referencing methods. This highlights that the ^{1}H-^{15}N HSQC spectrum of the chimera resembles a combination of the sTnI and sNTnC spectra both as seen in the troponin complex.

The backbone chemical shifts assignment was obtained using the 3D HNCACB, 3D HNCACO, 3D HNCO, and 3D ^{15}N NOESYHSQC NMR spectra. The backbone chemical shift assignment was completed to 80, 80, 82, 80, and 79% for the HN, N, CO, Cα, and Cβ nuclei, respectively. We have compared the chemical shifts of the sTnC and sTnI portions of the chimera with those of the respective proteins in the Tn complex (Fig. 4), after adjustment for the effect of the TROSY acquisition mode of the sTn chemical shifts. The HN, N and Cα chemical shifts of sTnC in the chimera revealed only minimum changes compared to those obtained previously for sNTnC in the Tn complex,[25] suggesting a high level of structural similarity. The small discrepancies for the Cα nucleus originate from the deuterated isotope shift in the sTn complex. The chemical shifts of the sTnI domain of the chimera were also similar to those of the C-terminal region of TnI in the ternary Tn complex (BMRB 9500).[11] These comparisons indicate that the structural characteristics of the IDR of TnI are virtually identical in the skeletal Tn

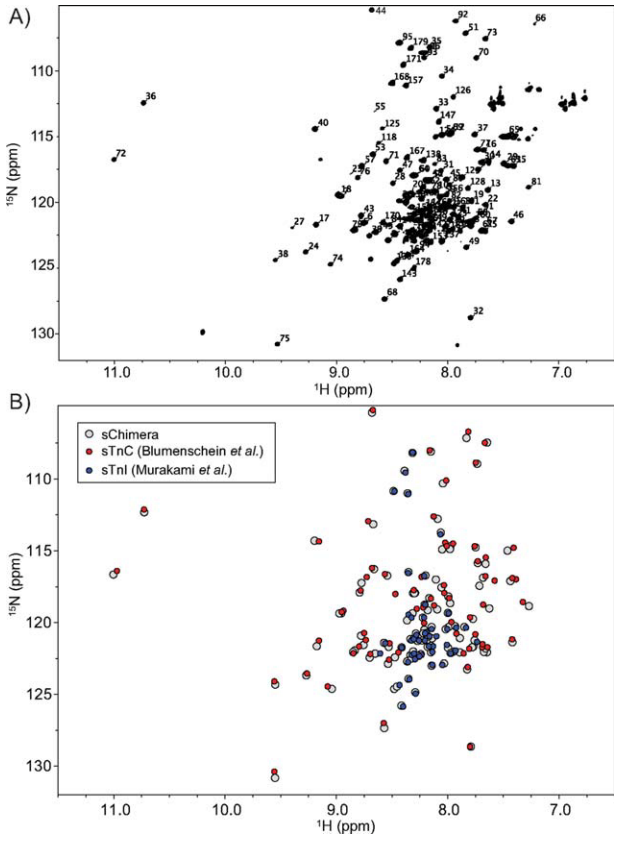

Figure 3

^{1}H-^{15}N-HSQC NMR spectrum of the skeletal TnC-TnI chimera. **A**: The cross-peaks are labeled with their corresponding residues. The spectrum was recorded at 30°C on an 800 MHz NMR spectrometer.
B: Superimposition of reconstructed ^{1}H-^{15}N HSQCs based on the chemical shifts of the chimera and the respective domains of TnC[25] and TnI[11] in the Tn complex. The chimera cross-peaks are colored grey, sTnC in red, and sTnI in blue. The resonances of the chimera not found in sTnC or sTnI were excluded for clarity, with most of them coming from the linker region.

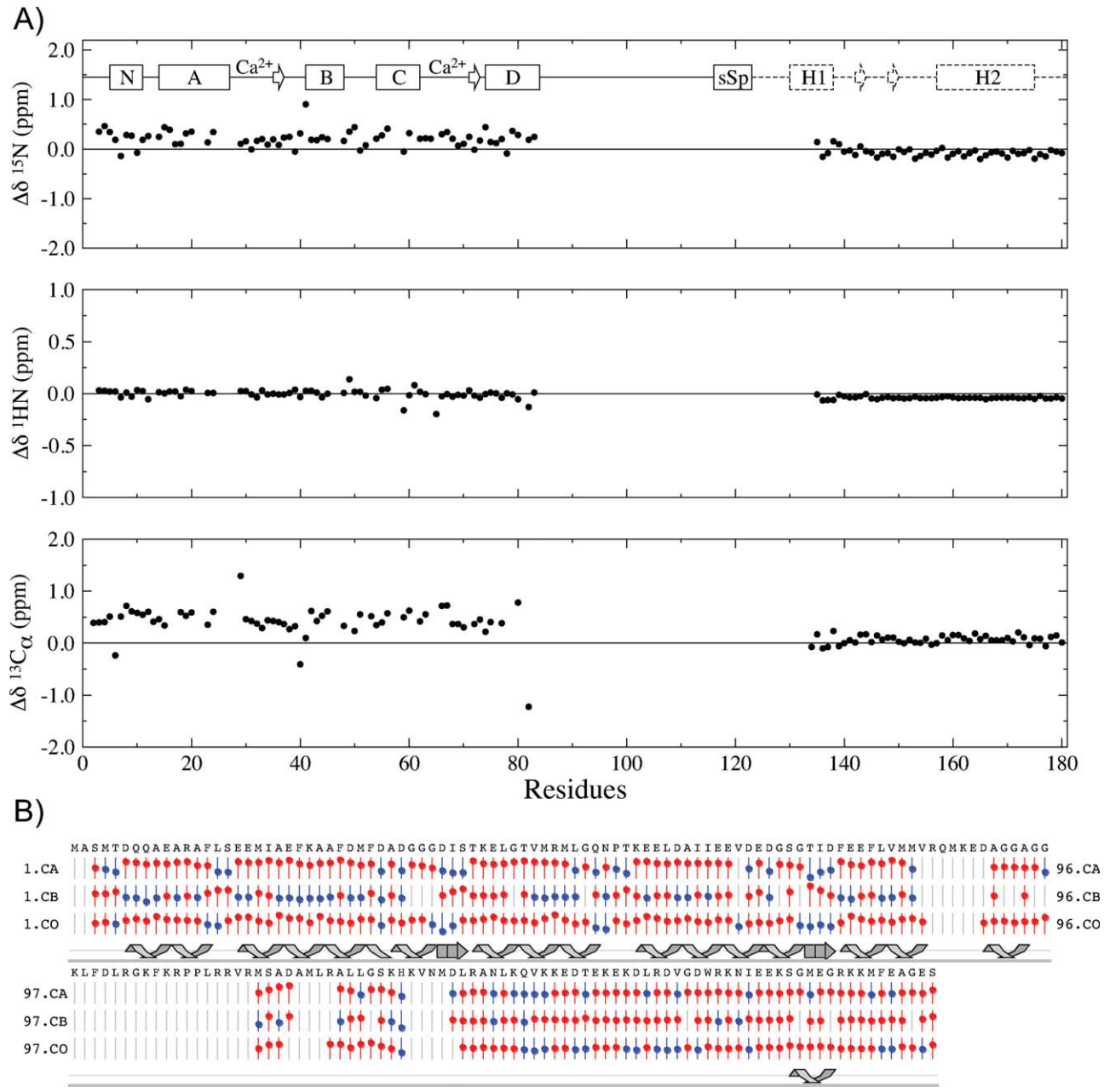

Figure 4

Chemical shifts of the skeletal TnC-TnI chimera. **A**: Chemical shift comparison between the chimera with sNTnC and sTnI. **B**: Chemical shift index (CSI) of the TnC-TnI chimera. The chemical shifts of the Cα, Cβ, and CO were used to calculate the secondary structure likelihood of each assigned residue. The chemical shifts were obtained from 3D HNCACB, CBCACONH, HNCO, and HNCACO experiments. [Color figure can be viewed in the online issue, which is available at wileyonlinelibrary.com.]

complex and in the TnC-TnI chimera used in this study. The ^{13}C chemical shifts (CO, Cα, and Cβ) of the chimera were used to calculate the chemical shift index (CSI)[26] to predict the secondary structure of the chimera in Figure 4(B). These results confirm the expected secondary structures for the sTnC domain but do not indicate any structure in the IDR of sTnI other than a short helix of five residues toward the end of the C-terminus.

NMR relaxation data

To assess the dynamic properties of the different regions of the chimera, we acquired the three standard backbone amide NMR relaxation experiments ^{15}N-T_1, ^{15}N-T_2, and $\{^1H\}^{15}N$-NOE at 600 and 800 MHz (Fig. 5). The ^{15}N-T_1 data for the sTnC region (residues 4–85) were 0.3 s higher at 800 MHz than at 600 MHz, with averages (± average errors) of 1.00 ± 0.03 s and 0.70 ±

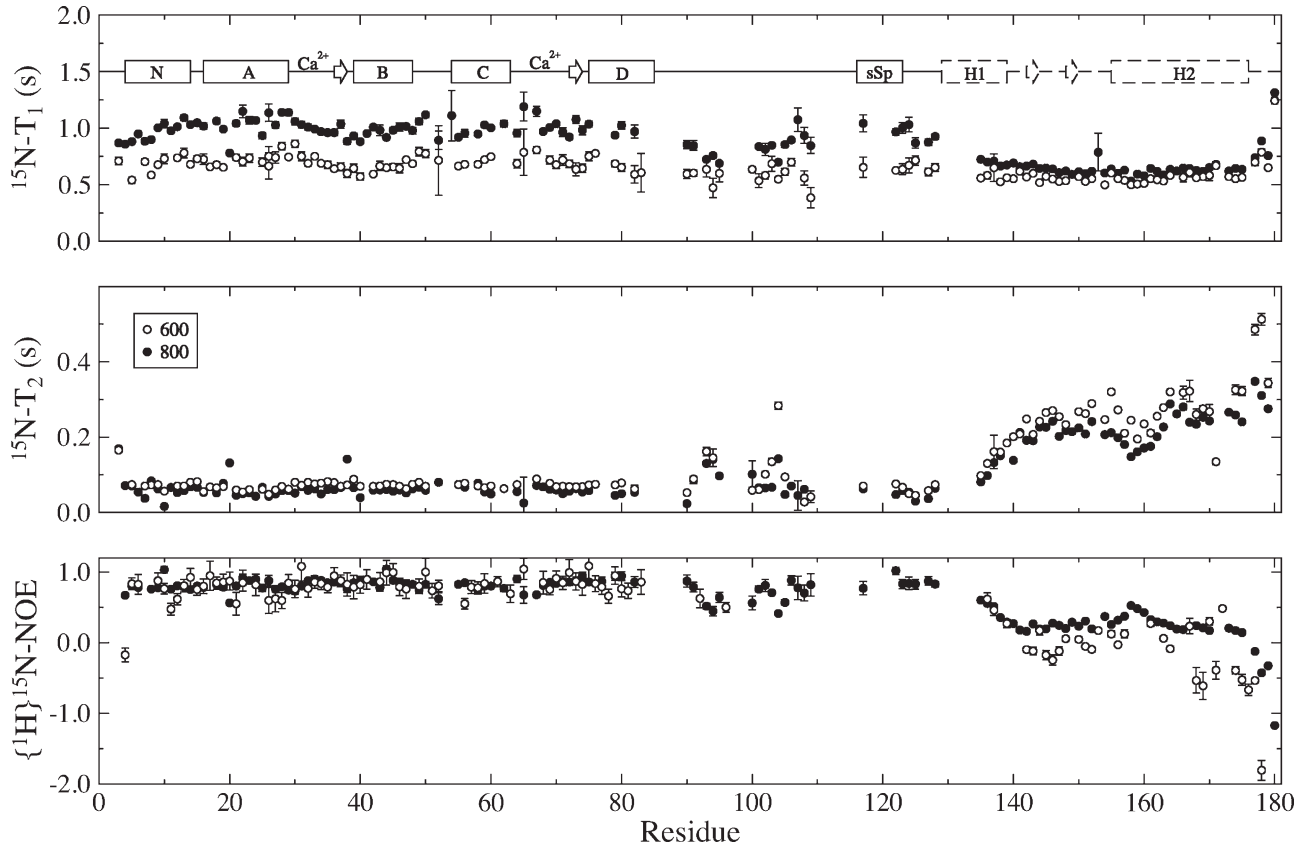

Figure 5

Backbone amide NMR relaxation parameters ^{15}N-T_1, ^{15}N-T_2, and {^{1}H}^{15}N-NOE of the skeletal TnC-TnI chimera. The data were measured at 600 MHz (white circles) and 800 MHz (black circles). The secondary structure elements of the chimera based on previous structures and chemical shift measurements presented in this article are shown with solid lines, whereas the previously proposed secondary structures proposed for the mobile domain are shown with dashed lines. Relaxation parameters for 10 residues visible in the ^{1}H-^{5}N HSQC but not unambiguously assigned were arbitrary attributed to residues 100–109 for graphing purposes.

0.04 s, respectively, as expected for a rigid globular domain. The ^{15}N-T_1 data for the C-terminal region of sTnI (residues 137–181), however, were similar at both fields (average of 0.57 ± 0.02 at 600 MHz, and 0.65 ± 0.02 at 800 MHz), characteristic of an IDR. The average ^{15}N-T_2 values at 600 MHz (800 MHz) for the sTnC and sTnI regions were 0.071 ± 0.004 (0.061 ± 0.003) and 0.258 ± 0.009 (0.215 ± 0.003), respectively. These values are typical for a globular domain for sTnC and a disordered region for the C-terminal region of sTnI. The ^{15}N-T_2 data show the presence of a "plateau" at approximately T_2 = 0.25 s for residues 140 to 170 of the IDR of sTnI, as observed for sTnI in the Tn complex.[6] Of particular interest, the average ^{15}N-T_2 at 600 MHz [800 MHz] for residues 124 to 130 of sTnI ($sTnI_{124–130}$) is 0.062 ± 0.005 s [0.049 ± 0.003 s]. These values for the switch region of sTnI are more similar to sTnC as opposed to sTnI (see discussion section for more details). The {^{1}H}^{15}N-NOE data reflects a well-folded protein for the sTnC region, with NOE values approaching 1.0, but dropping rapidly to lower values starting at residue 137 in the sTnI domain, suggesting a much more flexible region. Again, the NOE values for residues 124–130 of sTnI are more similar to the sTnC region, as opposed to the rest of the C-terminal region of sTnI. Overall, the ^{15}N-T_1, ^{15}N-T_2 and {^{1}H}^{15}N-NOE data obtained for the chimera are very similar to the experimental relaxation data for sTn,[6,25] justifying the use of the chimera to probe the motions of both regulatory domains when interacting to each other.

Molecular dynamics simulations

The validity of the different proposed models was assessed by molecular dynamic simulation using CHARMM. Four different trajectories using implicit solvent were acquired and 15 ns of each trajectory was analyzed to probe the motions of the chimera *in silico*. The correlation functions $C(t)$ of each residue in each model as a function of time are presented in the top panel of Figure 6(A–D). The correlation functions of the backbone amide NH vector reported are a measure of the mobility of a particular region; if the value of $C(t)$

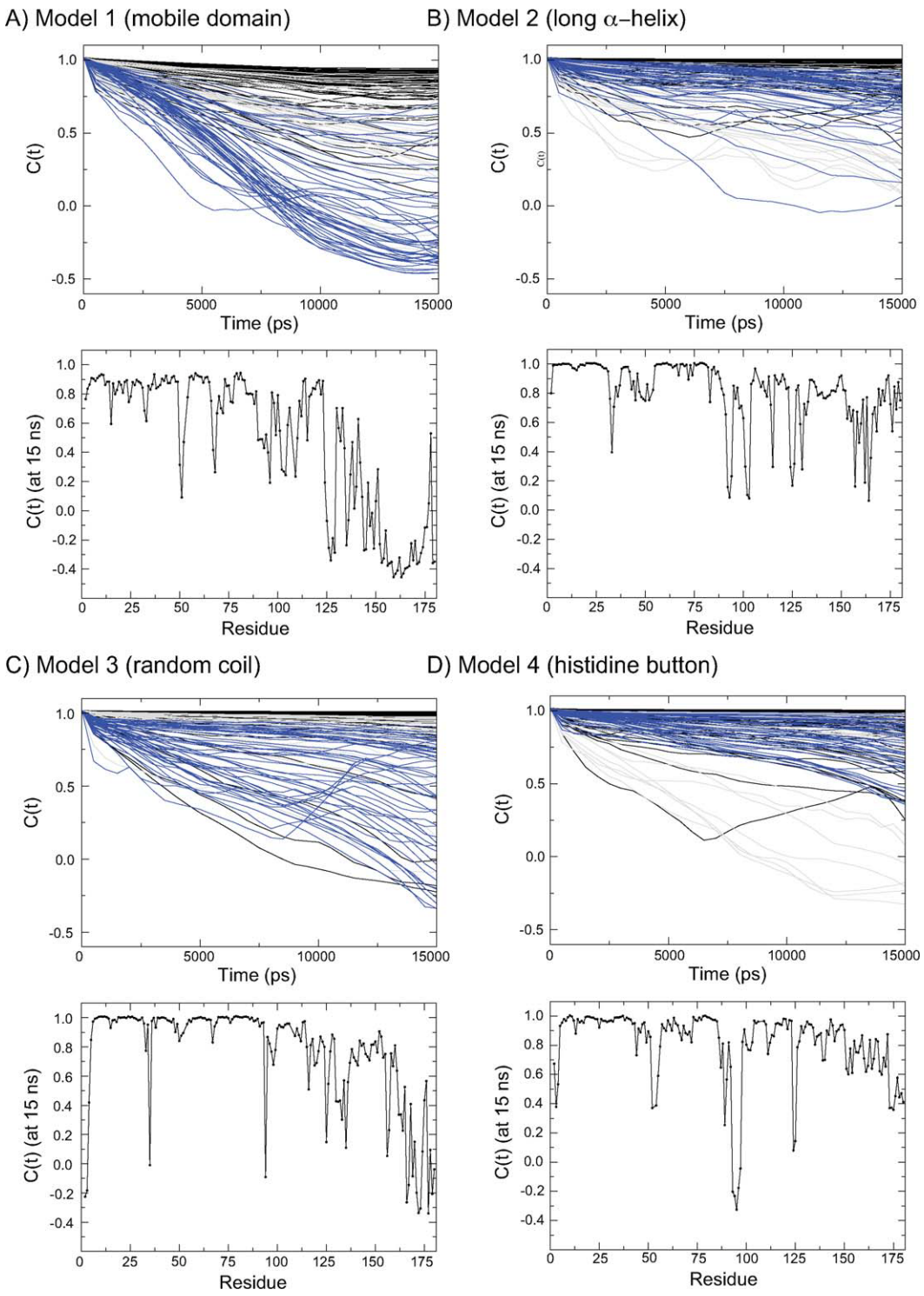

Figure 6

Correlation functions extracted from molecular dynamic simulations. **A**: Model 1, based of the mobile domain structure; **B**: Model 2, the helical model; **C**: Model 3, the flexible model; **D**: Model 4, the histidine button model. The figures at the top show the correlation functions as a function of correlation time, with residues 1–90 of sTnC colored in black, the linker and switch region of TnI colored in grey, and the C-terminal region of sTnI colored in blue. The graphs below show the amplitude of the correlation functions at 15 ns (estimated order parameter) as a function of residue number. The MD simulations were carried out using a Generalized Born with a simple switching (GBSW) implicit solvent model in CHARMM. The structures were first minimized, heated to 298 K, equilibrated, and followed by a 20 ns (or more) simulation for the analysis.

remains high this indicates that the motions of these residues are restricted. On the other hand, if the value of $C(t)$ decreases as a function of time, this indicates that the motions of a given residue are large on the time scale studied, and the conformation diverges over time. Of course, because the rotational reorientation of the TnC domain was removed before analysis (see Methods), $C(t)$ is close to one for residues in this domain that do not experience internal motions. Although the decays of the $C(t)$s for the individual residues are not labeled, the black band at the top of each panel corresponds to residues in the sTnC domain, and the ever more rapidly decaying curves correspond to residues in the C-terminus of the sTnI domain. To illustrate this, $C(t)$ is plotted on a per-residue basis at 15 ns in lower graphs for each model. These values of $C(t)$ reflect the order parameter of the internal motions of the chimera. The values close to 1.0 correspond to residue with limited backbone amide dynamics, observed for the rigid residues of the sTnC region in each model. For the sTnI region, the results show low-order reflecting considerable motion. Only model 4 predicts the correct position where the motion begins as seen in the experimental relaxation data (see below).

DISCUSSION

The chemical shifts of residues in the sTnC and sTnI regions of the chimera were virtually identical to those observed for both proteins when part of the full-length troponin complex.[6,25] Further, the dynamics of the chimera probed by ^{15}N NMR relaxation data also showed the same pattern as previously published. This supports the use of this chimera to characterize the structure and dynamics of the C-terminal region of TnI. The skeletal TnC-TnI chimera is also superior for all the technical reasons explained above, including enhanced stability (robustness to degradation over time) and NMR simplicity. We have used the ^{13}C chemical shifts as an indicator of secondary structure. Overall, the chemical shifts predict all expected secondary structure elements for the sTnC region, and point toward an IDR for the sTnI region, except for a short but possible nascent H2 helix as reported in the mobile domain structure.[11]

Two regions of the chimera revealed interesting relaxation data pattern. First, the "plateau" observed in the ^{15}N-T_1, ^{15}N-T_2 and $\{^1H\}^{15}$N-NOE NMR relaxation data for residues 140 to 170 of sTnI in the Tn complex[6] was also observed in the chimera. Although the relaxation data clearly show that this region is flexible, one possibility to explain the presence of the plateau is the presence of some sort of nascent structure. A second possibility is that this profile is an intrinsic property of disordered regions in general. We found that similar results can be recognized in other IDRs attached to globular domains using ^{15}N relaxation data, such as the data of Zhukov *et al.* who reported the ^{15}N NMR relaxation study of the ribosome-associated cold shock response protein Yfia.[27] This 90 amino acid protein structure corresponds to an antiparallel β-sheet with two α-helices positioned on the same side, with a 25 residues IDR at the C-terminus. The relaxation data measured at three different fields reveals a plateau of about 12 residues that resembles the one found in our relaxation data. In another case, Liu at al.[28] report backbone amide ^{15}N relaxation data for human PDCD5. The globular domain of 100 amino acids is mainly α-helical, while the C-terminus corresponds to an IDR of 30 residues that shows a clear plateau in all three NMR relaxation parameters.

The second region of interest consists of residues 124 to 130 of sTnI. The backbone dynamics of this region monitored by NMR relaxation show no evidence of mobility, with values of ^{15}N-T_1, ^{15}N-T_2, and $\{^1H\}^{15}$N-NOE more comparable with sTnC than to the flexible C-terminal region of sTnI. For example, the average ^{15}N-T_2 at 800 MHz for residues 124–130 of $sTnI_{124–130}$ (0.049) is similar to the sTnC region (0.061) as opposed to the C-terminal region of sTnI (0.215). This indicates that residues 124–130 of sTnI are as rigid as the globular domain of sTnC. The MD simulation for model 4 also reflects this experimental result. This observation was surprising, because these residues were not shown to be rigid in the NMR solution structure of the sNTnC:$sTnI_{115–131}$[29,30] as well as in the homologous cardiac structure.[31] This region of sTnI makes contact with α-helix A of sTnC in the X-ray structure of the sTn complex but with electronic density observable only in one of the two conformers seen in the crystal (chain I).[13] Importantly, the proximity of H130 of sTnI with E20 of sTnC was proposed to be a pH-dependent interaction known as a "histidine button" responsible for the pH sensitivity difference between skeletal and cardiac muscle, and, therefore, sensitivity to lactic acidosis generated in ischemic conditions.[32,33] Our experimental relaxation data for this region support this theory, and reveal that residues 124–130 are not flexible as previously interpreted.

All of the MD simulations show a gradient of correlations times for residues in the C-terminus but none of the simulations fit the details of the experimental NMR data. This can be seen in Figure 7 where the calculated relaxation parameters are compared with the experimental data. The relaxation data calculated for the N-terminal globular sTnC domain fit the experimental NMR relaxation parameters well, including the details of flexibility of the linker between the two calcium-binding sites.[34] However, the amplitude of the motions sampled in the MD simulations is never large enough to result in calculated data that reach the experimental data (see ^{15}N-T_2 in particular) nor is the plateau reproduced. Even the flexible model 3 featuring an absence of nascent secondary structure was not able to reproduce the mobility of the C-terminal region of TnI as seen in the

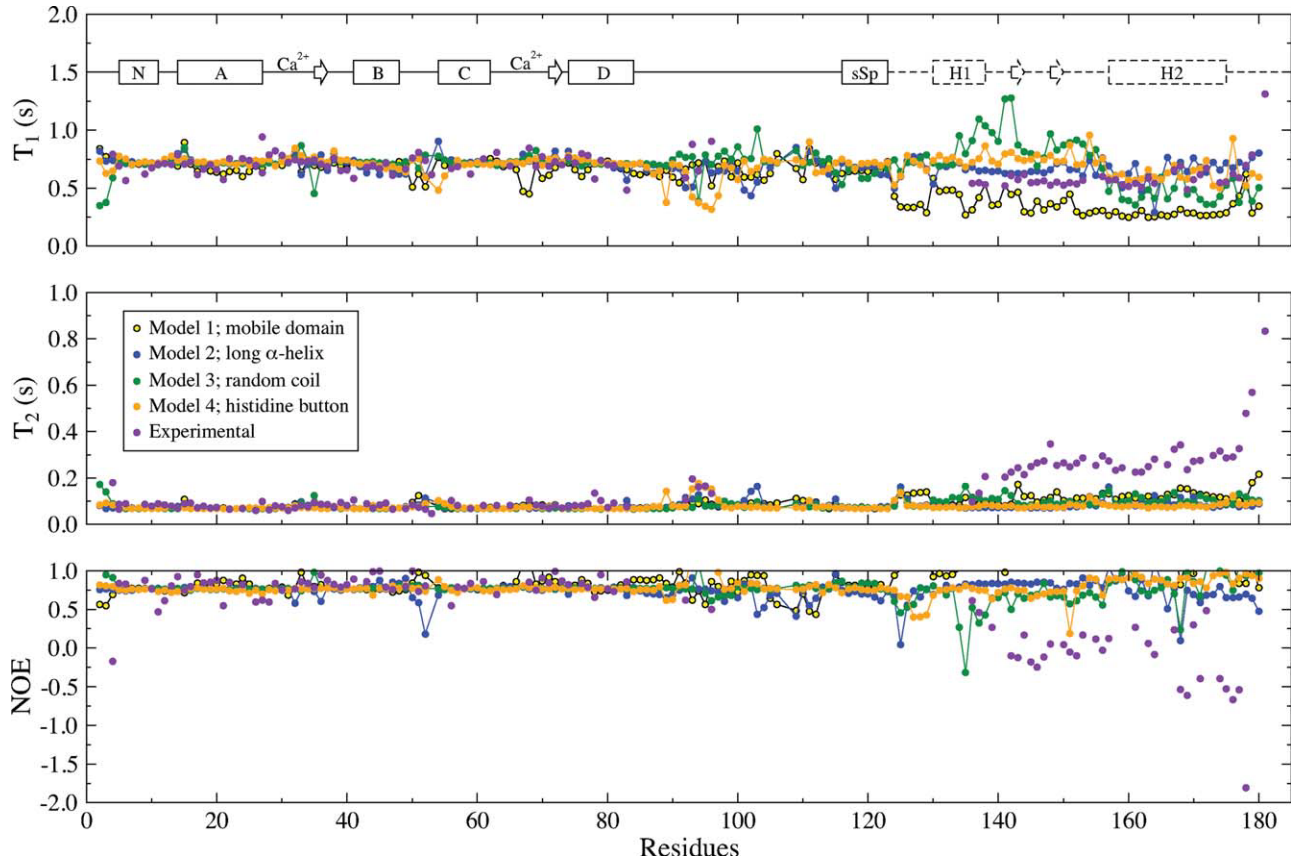

Figure 7

Comparison of the experimental NMR relaxation parameters ^{15}N-T_1, ^{15}N-T_2, and {^{1}H}^{15}N-NOE with the one calculated from the MD trajectories. The models 1–4 are colored in yellow, blue, green, and orange, respectively. Experimental data acquired at 600 MHz are shown in violet. An isotropic overall tumbling time of 10 ns for the chimera was assumed for the analysis.

experimental ^{15}N-T_2 NMR data. Although this could suggest that none of the models were appropriate, it more likely suggests that the molecular dynamic simulations used in this study were unable to reproduce the larger conformational sampling required to model the intrinsically disordered region of TnI.

CONCLUSION

Overall, our results indicate that the use of the sTnC-sTnI chimera is a good strategy to probe the dynamics of this key regulatory interaction within the sTn complex. Our relaxation data showed that the N-domain of sTnC is well folded and interacts with its sTnI binding partner in the chimera as expected. The NMR relaxation and chemical shift data of the C-terminal region of sTnI show the presence of a flexible and disordered region. Although standard MD simulations were successful in characterizing the internal motions within a globular domain of our construct, we were unable to reproduce the conformational sampling required to describe the large-scale motions of the intrinsically disordered region in detail. On balance, our experimental and MD data argues against any stable secondary structure significantly populated in the IDR of sTnI. This conclusion supports the role of a "fly-casting" mechanism for regulation of muscle contraction. The fact that a similar plateau in the relaxation data can be observed for other proteins suggests that this is an intrinsic property of extended mobile IDRs. We also observed an interaction of the region of sTnI immediately adjacent to the IDR with sTnC, which has important implications in the performance of skeletal muscle under ischemic conditions.

ACKNOWLEDGMENTS

The authors thank Dr. Leo Spyracopoulos for many insightful discussions. The authors also thank The Wolfson Foundation for its support to the UEA-Wolfson Molecular Structure Centre at the University of East Anglia, and the Canadian National High Field NMR Centre (NANUC) for their assistance and use of the facilities. The authors thank the Western Canada

Research Grid (WestGrid) for ample provision of CPU time on its supercomputers.

REFERENCES

1. Sykes BD. Pulling the calcium trigger. Nat Struct Biol 2003;10:588–589.
2. Gordon AM, Homsher E, Regnier M. Regulation of contraction in striated muscle. Physiol Rev 2000;80:853–924.
3. Tobacman LS. Thin filament-mediated regulation of cardiac contraction. Annu Rev Physiol 1996;58:447–481.
4. Farah CS, Reinach FC. The troponin complex and regulation of muscle contraction. FASEB J 1995;9:755–767.
5. Shoemaker BA, Portman JJ, Wolynes PG. Speeding molecular recognition by using the folding funnel: the fly-casting mechanism. Proc Natl Acad Sci USA 2000;97:8868–8873.
6. Blumenschein TM, Stone DB, Fletterick RJ, Mendelson RA, Sykes BD. Dynamics of the C-terminal region of TnI in the troponin complex in solution. Biophys J 2006;90:2436–2444.
7. Hoffman RM, Blumenschein TM, Sykes BD. An interplay between protein disorder and structure confers the Ca^{2+} regulation of striated muscle. J Mol Biol 2006;361:625–633.
8. Gomes AV, Potter JD. Cellular and molecular aspects of familial hypertrophic cardiomyopathy caused by mutations in the cardiac troponin I gene. Mol Cell Biochem 2004;263:99–114.
9. Lassalle MW. Defective dynamic properties of human cardiac troponin mutations. Biosci Biotechnol Biochem 2010;74:82–91.
10. Takeda S, Yamashita A, Maeda K, Maeda Y. Structure of the core domain of human cardiac troponin in the Ca^{2+}-saturated form. Nature 2003;424:35–41.
11. Murakami K, Yumoto F, Ohki SY, Yasunaga T, Tanokura M, Wakabayashi T. Structural basis for Ca^{2+}-regulated muscle relaxation at interaction sites of troponin with actin and tropomyosin. J Mol Biol 2005;352:178–201.
12. King WA, Stone DB, Timmins PA, Narayanan T, von Brasch AA, Mendelson RA, Curmi PM. Solution structure of the chicken skeletal muscle troponin complex via small-angle neutron and X-ray scattering. J Mol Biol 2005;345:797–815.
13. Vinogradova MV, Stone DB, Malanina GG, Karatzaferi C, Cooke R, Mendelson RA, Fletterick RJ. Ca^{2+}-regulated structural changes in troponin. Proc Natl Acad Sci USA 2005;102:5038–5043.
14. Cooke JA, Chamoun J, Howell MW, Curmi PM, Fajer PG, Brown LJ. Structure and Dynamics of the Mobile Domain of Troponin I by SDSL-EPR. Biophys J 2010;98:148A.
15. Tiroli AO, Tasic L, Oliveira CL, Bloch CJ, Torriani I, Farah CS, Ramos CH. Mapping contacts between regulatory domains of skeletal muscle TnC and TnI by analyses of single-chain chimeras. FEBS J 2005;272:779–790.
16. Baryshnikova OK, Williams TC, Sykes BD. Internal pH indicators for biomolecular NMR. J Biomol NMR 2008;41:5–7.
17. Delaglio F, Grzesiek S, Vuister GW, Zhu G, Pfeifer J, Bax A. NMRPipe: a multidimensional spectral processing system based on UNIX pipes. J Biomol NMR 1995;6:277–293.
18. Brooks BR, Bruccoleri RE, Olafson BD, States DJ, Swaminathan S, Karplus M. CHARMM: a program for macromolecular energy, minimization, and dynamics calculations. J Comput Chem 1983;4:187–217.
19. Sali A, Blundell TL. Comparative protein modelling by satisfaction of spatial restraints. J Mol Biol 1993;234:779–815.
20. Im W, Beglov D, Roux B. Continuum solvation model: computation of electrostatic forces from numerical solutions to the Poisson-Boltzmann equation. Comput Phys Commun 1998;111:59–75.
21. MacKerell AD, Bashford D, Bellott M, Dunbrack RL, Evanseck JD, Field MJ, Fischer S, Gao J, Guo H, Ha S, Joseph-McCarthy D, Kuchnir L, Kuczera K, Lau FTK, Mattos C, Michnick S, Ngo T, Nguyen DT, Prodhom B, Reiher WE, Roux B, Schlenkrich M, Smith JC, Stote R, Straub J, Watanabe M, Wiorkiewicz-Kuczera J, Yin D, Karplus M. All-atom empirical potential for molecular modeling and dynamics studies of proteins. J Phys Chem B 1998;102:3586–3616.
22. Mackerell AD, Feig M, Brooks CL. Extending the treatment of backbone energetics in protein force fields: limitations of gas-phase quantum mechanics in reproducing protein conformational distributions in molecular dynamics simulations. J Comput Chem 2004;25:1400–1415.
23. Im WP, Lee MS, Brooks CL. Generalized born model with a simple smoothing function. J Comput Chem 2003;24:1691–1702.
24. Abragam A. The principles of nuclear magnetism. Oxford: Clarendon Press; 1961.
25. Blumenschein TM, Stone DB, Fletterick RJ, Mendelson RA, Sykes BD. Calcium-dependent changes in the flexibility of the regulatory domain of troponin C in the troponin complex. J Biol Chem 2005;280:21924–21932.
26. Wishart DS, Sykes BD. The 13C chemical-shift index: a simple method for the identification of protein secondary structure using 13C chemical-shift data. J Biomol NMR 1994;4:171–180.
27. Zhukov I, Bayer P, Scholermann B, Ejchart A. 15N magnetic relaxation study of backbone dynamics of the ribosome-associated cold shock response protein Yfia of Escherichia coli. Acta Biochim Pol 2007;54:769–775.
28. Liu D, Feng Y, Cheng Y, Wang J. Human programmed cell death 5 protein has a helical-core and two dissociated structural regions. Biochem Biophys Res Commun 2004;318:391–396.
29. McKay RT, Tripet BP, Pearlstone JR, Smillie LB, Sykes BD. Defining the region of troponin-I that binds to troponin-C. Biochemistry 1999;38:5478–5489.
30. Mercier P, Ferguson RE, Irving M, Corrie JET, Trentham DR, Sykes BD. NMR structure of a bifunctional rhodamine labeled N-domain of troponin C complexed with the regulatory "switch" peptide from troponin I: implications for in situ fluorescence studies in muscle fibers. Biochemistry 2003;42:4333–4348.
31. Li MX, Spyracopoulos L, Sykes BD. Binding of cardiac troponin-I147–163 induces a structural opening in human cardiac troponin-C. Biochemistry 1999;38:8289–8298.
32. Dargis R, Pearlstone JR, Barrette-Ng I, Edwards H, Smillie LB. Single mutation (A162H) in human cardiac troponin I corrects acid pH sensitivity of Ca^{2+}-regulated actomyosin S1 ATPase. J Biol Chem 2002;277:34662–34665.
33. Day SM, Westfall MV, Fomicheva EV, Hoyer K, Yasuda S, La Cross NC, D'Alecy LG, Ingwall JS, Metzger JM. Histidine button engineered into cardiac troponin I protects the ischemic and failing heart. Nat Med 2006;12:181–189.
34. Gagné SM, Tsuda S, Spyracopoulos L, Kay LE, Sykes BD. Backbone and methyl dynamics of the regulatory domain of troponin C: anisotropic rotational diffusion and contribution of conformational entropy to calcium affinity. J Mol Biol 1998;278:667–686.